Eur. Phys. J. B **23**, 283–296 (2001)

THE EUROPEAN PHYSICAL JOURNAL B

EDP Sciences

Magnetoquantum de Haas-van Alphen oscillations in spin-split two-dimensional Fermi liquid

M.A. Itskovsky[a]

Technion-Israel Institute of Technology, Department of Chemistry, Haifa 32000, Israel

Received 20 December 2000 and Received in final form 13 July 2001

Abstract. Theory of magnetoquantum oscillations with spin-split structure in strongly anisotropic (two-dimensional (2D)) metal is developed in the formalism of level approach. Parametric method for exact calculation of oscillations wave forms and amplitudes, developed earlier for spin degenerate levels is generalized on a 2D electron system with spin-split levels. General results are proved: 1) proportionality relation between magnetization and chemical potential oscillations accounting for spin-split energy levels and magnetic field unperturbed levels (states of reservoir), 2) basic equation for chemical potential oscillations invariant to various models of 2D and 1D energy bands (intersecting or overlapping) and localized states. Equilibrium transfer of carriers between overlapping 2D and 1D bands, characterizing the band structure of organic quasi 2D metals, is considered. Transfer parameter, calculated in this model to be of the order of unity, confirms the fact that *the wave form of oscillations in organic metals should be quasisymmetric up to ultralow temperature.* Presented theory accounts for spin-split magnetization oscillations at magnetic field directions tilted relative to the anisotropic axis of a metal. Theoretical results are compared with available experimental data on organic quasi-2D metal α-(BEDT-TTF)$_2$KHg(SNC)$_4$ explaining the appearance of clear split structure under the kink magnetic field and absence above by the corresponding change in the electron g-factor rather than cyclotron mass.

PACS. 75.20.-g Diamagnetism, paramagnetism, and superparamagnetism – 75.20.En Metals and alloys – 75.30.Cr Saturation moments and magnetic susceptibilities

1 Introduction

Magnetoquantum oscillations in metals under high quantizing magnetic field (de Haas-van Alphen (dHvA) and Shubnikov-de Haas (SdH) effects) are widely utilized for obtaining essential identity properties of metals: topology of Fermi surface and constituent band structure parameters such as effective band masses and Fermi energy [1]. Appropriate cyclotron mass, m_c, can be extracted from temperature dependence of oscillations amplitudes, the Fermi energy – from measurements of fundamental frequency of oscillations. Spin-splitting of quantum energy levels (Landau levels (LL)) leads to the characteristic spin-split structure of oscillations and can reveal such property as electron g-factor.

Magnetization and resistance oscillations with spin-split structure were revealed in a number of experiments on organic quasi-two-dimensional (2D) metals [2,3], especially with magnetic field direction being tilted relative to the anisotropic axis [4] of a metal. Clear spin-split structure has been observed in organic conductor α-(ET)$_2$KHg(SNC)$_4$ [5–7] (ET further on stands for BEDT-TTF). Recently spin-splitting around the high magnetic field phase transition in this organic metal (around the kink field of about $B_K = 23$ T) was investigated and values of the parameter gm_c/m_e under and above transition field were established [8] (m_e is the electron mass). Magnetization oscillations with weakly shown spin-split structure at ultralow temperature ($T = 0.035$ K) (maybe due to the small angle in the torque experiment ($\Theta = 3°$) [9] and partly to the relatively high Dingle temperature in the samples used) was observed in organic metal $\kappa - (ET)_2I_3$ in reference [10], the wave form of spin-split magnetization being interpreted by the numerical fit for the ensemble of quantized carriers, not accounting for the reservoir of carriers on magnetic field independent levels.

Pronounced spin-split structure was reported in our work [11] on organic metal $\kappa - (ET)_2I_3$ at tilt angles near first spin-splitting zero. In that work the conditions for the appearance of spin-split structure (corresponding temperature, magnetic field and spin-splitting of energy levels) were determined. Spin-split structure arises more clearly in pure samples (those with low Dingle temperature), at ultralow temperature where the parameter for temperature smoothing $Q = \hbar\omega_c/k_BT$ ($\omega_c = eB/m_cc$ is the cyclotron frequency, B is the magnetic induction) becomes relatively large, for tilt angles providing the substantial magnitude of the spin-splitting parameter $s = \Delta_s/\hbar\omega_c$ (Δ_s is the energy difference between nearest levels with spin up

[a] e-mail: chr40im@techunix.technion.ac.il

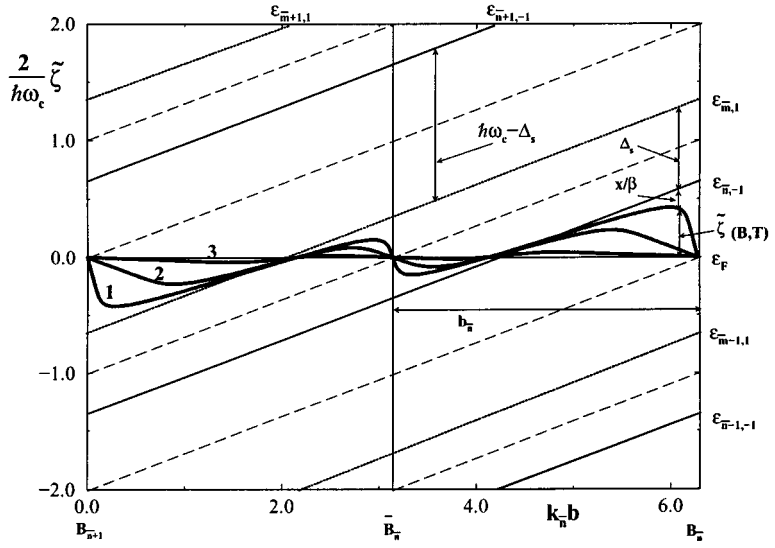

Fig. 1. Chemical potential oscillations in a 2D metal with spin-split Landau levels. Chemical potential oscillations are drawn according to the parametric equations (23–25) for transfer parameter, c_R: curve 1: $c_R = 0.1$, curve 2: 1.0, curve 3: 10. Spin-split levels are drawn according to equations (2, 3): levels with spin projections along magnetic field are shown by solid lines, those with spin opposite to the field – by dotted lines, middles between levels – by dashed lines (6 spin-split levels are shown sufficient for exact calculation of the magneto-quantum oscillations in the entire region of spin-splitting parameter $0 \leqslant s \equiv \Delta_s/\hbar\omega_c \leqslant 0.5$ and temperature smoothing parameter $Q \equiv \hbar\omega_c/k_BT \gtrsim 5$). Singled period constrained by magnetic fields $B_{\bar{n}+1} \equiv B_{\bar{n}+1,\bar{m}}$ and $B_{\bar{n}} \equiv B_{\bar{n},\bar{m}-1}$ is shown. Center of period at field $\bar{B}_{\bar{n}} \equiv B_{\bar{m},\bar{n}}$ is shown by the vertical line, $b_{\bar{n}} = B_{\bar{n}+1}B_{\bar{n}}/2F$ is half-period, $b = B - B_{\bar{n}}$, $k_{\bar{n}} = \pi/b_{\bar{n}}$ is the cyclic frequency relative to magnetic field. Energies are drawn in the $\hbar\omega_c/2$ units: $x(b,T)/\beta = \varepsilon_{\bar{n},-1} - \zeta(B,T)$ ($x(b,T)$ is the parametric variable), $\tilde{\zeta}(B,T) = \zeta(B,T) - \varepsilon_F$ is the chemical potential oscillations, $\Delta_s = \varepsilon_{\bar{m},1} - \varepsilon_{\bar{n},-1}$ is the spin-splitting energy (difference between nearest levels with opposite spin projections). Fermi level, ε_F, is shown as zero line. Here the temperature smoothing parameter is $Q = 44$, the spin-splitting parameter is $s = 0.35$. Note the suppression of the chemical potential oscillations with increasing of the transfer parameter, c_R. Note also the symmetry of levels dispositions relative to the Fermi level at the ends and the center of period.

and down (see Fig. 1), $m_c = m_{c0}/\cos\Theta$ is the cyclotron mass at tilt angle Θ, m_{c0} is the cyclotron mass at $\Theta = 0$). However, the wave forms of spin-split oscillations in the formalism of level approach which stems from the work of Peierls [12] (direct summation on symmetric electron and hole pairs of spin-split levels around Fermi level in any period of oscillations) were not considered. In the high magnetic field-low temperature region analysis based on Lifshitz-Kosevich (LK) formulae is inefficient: formalism of harmonic approach (LK harmonics series) neglecting the chemical potential oscillations gives inverse sawtooth wave form at ultralow temperature, characteristic of constant chemical potential [13] which is not generally the case in 2D organic metals. Recently spin-split oscillations at $T = 0$ were considered in the formalism of harmonic approach, the electron reservoir (background) states explicitly being taken into account [14] (see also [15,16]).

Here we will develop theory of wave forms of spin-split magnetization oscillations for a 2D electron system containing both spin-split quantum levels and magnetic field independent levels of reservoir at arbitrary temperature. Simple analytical formulae in the formalism of level approach will be derived describing magnetization wave forms with spin-split structure in the entire magnetic field-temperature region corresponding to the temperature smoothing parameter $Q \gtrsim 1$. The obtained analytical results will be valid in the interval of quantizing magnetic fields satisfying the conditions: $k_BT \lesssim \hbar\omega_c(B) \lesssim \varepsilon_F$ (ε_F is the Fermi energy counted from the bottom of quantized band).

We will prove the *ab initio* not obvious fact that general proportionality relationship between magnetization and chemical potential oscillations [17] exists independently of spin-degenerate or spin-split energy levels and the equilibrium exchange of quantized carriers with those on field independent levels. This exchange does not influence magnetization amplitudes which are the subject to suppression by the other reasons: by the increasing temperature, level broadening, etc. The similar suppression concerns the spin-split structure, its shape also being determined by the equilibrium transfer of carriers between quantum and field independent levels. We will generalize the parametric method derived in reference [17] for a system with spin-split levels. The basic equation for chemical potential oscillations determining the shape of magneto-quantum oscillations will be shown to be invariant relative to the various models of energy bands in 2D metals (intersecting or overlapping) and presence of localized states. Here we consider model of overlapping 2D and 1D bands characteristic of organic 2D metals (in Refs. [17,18] the model of intersecting bands was elaborated).

It should be noted that in the semiclassical theory of magnetoquantum oscillations applied here the correlation between electrons is taken into account in a way as it is done in the Fermi liquid concept, through the notion of effective (cyclotron) mass entering into the quasiparticle spectrum of conduction electrons of a metal [19]. The applicability of semiclassical approach to description of magnetoquantum oscillations in 2D metals was demonstrated by comparing the semiclassical LK formulae with numerical microscopic quantum-mechanical calculations for determining the effective mass [20–22].

In Section 2 we consider in the formalism of level approach the general expression for magnetization and basic equation for chemical potential oscillations, both accounting for spin-split quantum levels and magnetic field independent states of reservoir. The model of overlapping 2D and 1D bands is elaborated.

In Section 3 we apply the parametric method for calculating the exact wave form of oscillations accounting for spin-splitting of discrete quantum levels. We compare these wave forms with those obtained *via* the LK formulae adapted for 2D electron systems by Shoenberg (LKS formula [23]) and at ultralow temperature with Nakano formula [14] accounting for reservoir states at $T = 0$. We compare theoretical shapes of magnetization oscillations with experimental ones around kink magnetic field in organic metal α-$(ET)_2KHg(SNC)_4$.

2 Basic relations for spin-split oscillations in a 2D metal. Model of overlapping 2D and 1D bands

Thermodynamic potential of spin-split Fermi liquid in a 2D metal (ensemble of electrons being situated on spin-split levels of the 2D subband and moving under high magnetic field on quantized closed orbits) can be written as [24,25]:

$$\frac{\Omega_{\rm LL}(B,\zeta)/V}{A} = -\frac{B}{\beta}\left[\sum_{n=0}\frac{1}{2}\ln\left(1+\exp[(\zeta-\varepsilon_{n,-1}(B))\beta]\right) + \sum_{m=0}\frac{1}{2}\ln\left(1+\exp[(\zeta-\varepsilon_{m,1}(B))\beta]\right)\right], \quad (1)$$

where $A \equiv 2\cos\Theta/c^*\phi_0$, $\phi_0 = hc/e$ is the flux quantum, $\beta \equiv 1/k_{\rm B}T$, c^* is the lattice constant in the anisotropic k_z-direction of a metal, Θ is the angle between the anisotropic axis $\mathbf{c}^*$ and the magnetic induction vector $\mathbf{B}$, ζ is the chemical potential generally dependent on magnetic field, V is the crystal volume.

Energy spectrum of quantized carriers is represented by the spin-split Landau levels, those with spin oriented along magnetic field:

$$\varepsilon_{n,-1}(B) = \hbar\omega_{\rm c}(B)(n+1/2) - \frac{1}{2}\frac{g}{2}\hbar\omega_{\rm e}(B), \quad n = 0,1,2,\cdots, \quad (2)$$

and those with spin oriented opposite magnetic field:

$$\varepsilon_{m,1}(B) = \hbar\omega_{\rm c}(B)(m+1/2) + \frac{1}{2}\frac{g}{2}\hbar\omega_{\rm e}(B), \quad m = 0,1,2,\cdots, \quad (3)$$

where $\hbar\omega_{\rm c}(B)=\mu_{\rm c}B$ is the levels separation corresponding to the cyclotron mass ($\mu_{\rm c} \equiv {\rm e}\hbar/m_{\rm c}c$), $\omega_{\rm e}(B) = eB/m_{\rm e}c$ is the cyclotron frequency corresponding to the electron mass, $m_{\rm e}$.

The intersections of these quantum levels on varying the magnetic field with the Fermi level, $\varepsilon_{\rm F}$, lead to the effect of magnetoquantum oscillations in a metal (see Fig. 1).

Let us separate any single quasiperiod by magnetic fields between which two nearest levels with fixed quantum numbers, $\bar{n}$ and $\bar{m}$, and opposite orientation of spin cross the Fermi level, $\varepsilon_{\rm F}$ (see Fig. 1): $B_{\bar{n}+1} \equiv B_{\bar{n}+1,\bar{m}} \leqslant B \leqslant B_{\bar{n}} \equiv B_{\bar{n},\bar{m}-1}$. Field $B_{\bar{n},\bar{m}-1} \equiv B_{\bar{n}}$ at the right end of the period (and similar field $B_{\bar{n}+1,\bar{m}} \equiv B_{\bar{n}+1}$ at the left end of the period) is defined so that at this field Fermi level is situated on the equal distance from the two successive levels with opposite spin:

$$[\varepsilon_{\bar{n},-1}(B_{\bar{n}}) + \varepsilon_{\bar{m}-1,1}(B_{\bar{n}})]/2 = \varepsilon_{\rm F}, \quad (4)$$

so that local symmetry of these levels relative to the Fermi level at this magnetic field holds. The similar relation holds for the left end of quasiperiod at field $B_{\bar{n}+1}$. At the middle of the period we define in a similar way the magnetic field, $B_{\bar{m},\bar{n}} \equiv \bar{B}_{\bar{n}}$, where two nearest levels with opposite spin orientation, $\bar{n}$ and $\bar{m}$, are situated on equal distances from the Fermi level:

$$[\varepsilon_{\bar{n},-1}(\bar{B}_{\bar{n}}) + \varepsilon_{\bar{m},1}(\bar{B}_{\bar{n}})]/2 = \varepsilon_{\rm F}. \quad (5)$$

Using the definition of spin-split levels, equations (2) and (3), we can introduce the spin-splitting parameter [11]:

$$s(G) \equiv \frac{\Delta_{\rm s}}{\hbar\omega_{\rm c}} = |G - I(G)|, \qquad G \equiv (g/2)(m_{\rm c}/m_{\rm e}), \quad (6)$$

where the energy difference between the two nearest spin-split levels with opposite spin projections (the spin-splitting energy) is (see Fig. 1):

$$\Delta_{\rm s} \equiv |\varepsilon_{\bar{n},-1} - \varepsilon_{\bar{m},1}|, \quad (7)$$

and

$$I(G) = [G] = \bar{n} - \bar{m}\ , \quad I = 0,1,2,... \quad (8)$$

is the nearest integer to the value of G (the designation $[G]$ stands here for the nearest integer to the value of G: for example, for $G = 4.8$, $I = 5$, for $G = 4.2$, $I = 4$; in both cases spin-splitting parameter is $s = 0.2$). From its definition, equation (6), it is clear that spin-splitting parameter ranges in the limits $0 \leqslant s \leqslant 0.5$ at all values of the parameter G. For an integer value of G the spin-splitting parameter is zero and high-lying spin-split levels are coinciding (the degeneracy of quantized levels relative

to spin projection), only in the case of $g \equiv 0$ *all* levels are degenerate (namely this particular case is usually considered in the theory of magnetoquantum oscillations in 2D metal [17,18,26]). For half-integer values of G the spin-splitting parameter is maximal ($s = 0.5$) and the spin-split levels are equidistant with energy separation equal to $\hbar\omega_c/2$. Hence, the spin-splitting parameter is a periodical function of the argument G with period equal to unity: $s(G) = s(G+1)$.

The basic equation for the chemical potential oscillations $\tilde{\zeta}(B) = \zeta(B) - \varepsilon_F$ for the model of intersecting 2D and 1D bands (including the electrons on localized levels) in accounting for spin-splitting of Landau levels may be written (derivation similar to that done in the Ref. [17]: see Appendix):

$$\frac{F}{B} - \frac{F}{B_{\bar{n}}} = -\frac{b}{2b_{\bar{n}}} = g_s(x,Q) + c_R\frac{\tilde{\zeta}(b)}{\hbar\omega_c},$$
$$c_R \equiv \mu_c[\partial n_R(\zeta)/\partial\zeta]_{\varepsilon_F}/A, \qquad (9)$$

where F is the fundamental frequency of oscillations relative to the inverse magnetic field ($1/F = 1/B_{\bar{n}+1} - 1/B_{\bar{n}}$, see Fig. 1), magnetic field is counted from the $B_{\bar{n}}$, $b = B - B_{\bar{n}}$, $b_{\bar{n}} = B_{\bar{n}+1}\ B_{\bar{n}}/2F = \pi/k_{\bar{n}}$ is half period of oscillations [$k_{\bar{n}} = 2\pi F/B_{\bar{n}+1}B_{\bar{n}}$ is the cyclic fundamental frequency relative to the magnetic field difference, $b = B - B_{\bar{n}}$]. Equation for the chemical potential oscillations (Eq. (9)) is fulfilled for every quasiperiod $B_{\bar{n}+1} \leqslant B \leqslant B_{\bar{n}}$ or $-2b_{\bar{n}} \leqslant b \leqslant 0$. The transfer parameter c_R is determined by the density of electrons filling the magnetic field independent levels of the reservoir: $n_R(\zeta) = n_{sh}(\zeta) + n_A(\zeta)$ ($n_{sh}(\zeta)$ is the concentration of free electrons situated on the open electron-like orbits (around open 1D Fermi surface sheet), $n_A(\zeta)$ is the concentration of localized electrons on the acceptor levels of impurities or defects). Here we do not take into account the possible dependence of the transfer parameter c_R on chemical potential oscillations $\tilde{\zeta}(b)$ which may be due to the omitting terms of the expansion of $n_R(\varepsilon_F + \tilde{\zeta})$ on $\tilde{\zeta}$, except of the linear. This transfer parameter is independent of the tilt angle of the magnetic field relative to the anisotropic axis, as it should be for the thermal (equilibrium) exchange of quantized and nonquantized carriers between different energy bands and/or localized states. In the case of spin-split levels the g-function entering into the equation for chemical potential oscillations (Eq. (9)) will be:

$$g_s(x,Q) = g_{-1}(x,Q) + g_1(x+sQ,Q),$$
$$g_{-1}(x,Q) \equiv \frac{1/2}{1+\exp(x)} + \sum_{k=1}^{\bar{n}}\left[\frac{1/2}{1+\exp(kQ+x)} - \frac{1/2}{1+\exp(kQ-x)}\right]$$
$$= \frac{1/2}{1+\exp(x)} - \sum_{k=1}^{\bar{n}}\frac{(1/2)\sinh x}{\cosh x + \cosh(kQ)},$$

$$g_1(x+sQ,Q) \equiv \frac{1/2}{1+\exp(x+sQ)} + \sum_{k=1}^{\bar{m}}\left[\frac{1/2}{1+\exp[kQ+(x+sQ)]} - \frac{1/2}{1+\exp[kQ-(x+sQ)]}\right]$$
$$= \frac{1/2}{1+\exp(x+sQ)} - \sum_{k=1}^{\bar{m}}\frac{(1/2)\sinh(x+sQ)}{\cosh(x+sQ)+\cosh(kQ)}, \qquad (10)$$

where $x(B,T) \equiv [\varepsilon_{\bar{n},-1}(B) - \zeta(B,T)]/k_BT$, $Q \equiv \hbar\omega_c/k_BT$.

At magnetic fields $B_{\bar{n}}$ and $B_{\bar{n}+1}$ the chemical potential crosses the Fermi level, so as at field, $\bar{B}_{\bar{n}}$, where the average curve between separated levels $\varepsilon_{\bar{n},-1}$ and $\varepsilon_{\bar{m},1}$ intersects with Fermi level (see Fig. 1). At these magnetic fields the energy levels can be arranged symmetrically relative to the Fermi level so that at the center of period where $x(\bar{B}_{\bar{n}}) = -(s/2)Q$ the function $g_s(-(s/2)Q,Q) = 1/2$, at the right end of the period where $x(B_{\bar{n}}) = Q(1-s)/2$ the function $g_s(Q(1-s)/2,Q) = 0$ and at the left end of the period where $x(B_{\bar{n}+1}) = -Q(1+s)/2$ the function $g_s(-Q(1+s)/2,Q) = 1$. Hence, the function $g_s(x,Q)$ plays the role of the effective filling of the two nearest spin-split levels, $\varepsilon_{\bar{n},-1}$ and $\varepsilon_{\bar{m},1}$, in total: at magnetic field $B_{\bar{n}}$ they are empty, at $\bar{B}_{\bar{n}}$-half-filled, at $B_{\bar{n}+1}$-filled. These values of the $g_s(x,Q)$-function do not depend on the parameter Q, *i.e.*, do not depend on temperature for the magnetic fields $B_{\bar{n}+1}$, $\bar{B}_{\bar{n}}$, $B_{\bar{n}}$. These values of the $g_s(x,Q)$-function are completely determined by the symmetrical dispositions of levels relative to the Fermi level at these magnetic fields. The two other remaining intersections of the chemical potential with Fermi level inside the separated period do depend on temperature (through the parameter Q) (see Fig. 1). In the case of spin-degenerate levels the latter intersections are absent: they coalesce simultaneously with nearest $\varepsilon_{\bar{n},-1}$ and $\varepsilon_{\bar{m},1}$ levels with the intersection at the center of period at magnetic field $\bar{B}_{\bar{n}}$. On $s = 0$ the $g_s(x,Q)$-function certainly coincides with the $g(x,Q)$-function defined for the spin-degenerate levels in reference [17].

The equation for chemical potential oscillations in the guise of equation (9) is written in the invariant form relative to the band structure of a metal and presence of localized states. In the case of overlapping 2D and 1D bands (see Fig. 2) we obtain the same equation for chemical potential oscillations, equation (9), but with transfer parameter

$$c_R^{(ov)} = \mu_c|\partial p_{sh}(\zeta)/\partial\zeta|_{\varepsilon_F}/A, \qquad (11)$$

where $p_{sh}(\zeta)$ is the hole concentration in the 1D band (inside the 1D Fermi surface sheet).

Case of overlapping bands is appropriate to the even number of valence electrons on a unit cell, the concentration of electrons and holes in corresponding subbands being arbitrary but equal. The concentration is determined

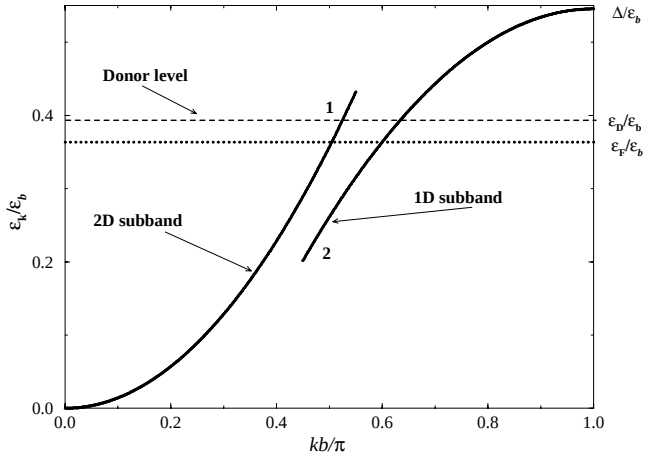

Fig. 2. Model of overlapping bands. Two-dimensional (2D) and one-dimensional (1D) subbands dispersion relations in the direction normal to the planar 1D Fermi surface sheet, drawn according to parabolic dispersion near the corresponding extrema in the $k_y \equiv k$-direction: $\varepsilon_k^{(2D)} = \hbar^2 k^2/2m_{c0}$ and $\varepsilon_k^{(1D)} = \Delta - \hbar^2(\pi/b - k)^2/2|m_{sh}|$. Δ is the subbands overlapping energy, ε_F is the Fermi energy; energies are counted from the bottom of the 2D subband and are represented in $\varepsilon_b \equiv \hbar^2(\pi/b)^2/2m_e$ units ($\varepsilon_b \cong 308$ meV if $b = 10$ Å). At values of $\Delta \cong 168$ meV and $\varepsilon_F \cong 112$ meV (calculated for α-$(ET)_2KHg(SNC)_4$ organic metal in Ref. [27]) the ratios $\Delta/\varepsilon_F \cong 1.5$, $\Delta/\varepsilon_{ef} \cong 0.75$ and according to the equation (19) the transfer parameter in this case is $c_R^{(ov)} \cong 1.0$. Dispersion in subbands is drawn for $m_{c0}/m_e = m_b/m_e = 0.7$ and $|m_{sh}|/m_e = 0.9$ consistent with the above values of Δ and ε_F (m_b is the effective band mass for 2D subband (without account for many-body electron-electron and electron-phonon interactions, see Ref. [1])). The donor level, ε_D, is represented by the dashed line, the Fermi level, ε_F, by the dotted line.

by the overlapping energy, Δ, the energy difference between top of the 1D subband and the bottom of the 2D subband (see Fig. 2). In a case of Δ being positive and $\Delta \gg k_B T$ the carriers inside subbands will be degenerate and the magnetoquantum oscillations will be sufficiently large for observation. The equation for the chemical potential in the model of overlapping bands is:

$$p_{sh}(\zeta) = n_{LL}(B, \zeta), \tag{12}$$

where $n_{LL}(B, \zeta)$ is the concentration of electrons on quantized levels in the electron-like pocket of the 2D band.

Expanding the hole concentration in a series of $\tilde{\zeta}$,

$$p_{sh}(\zeta) = p_{sh}(\varepsilon_F) + \partial p_{sh}/\partial\zeta|_{\varepsilon_F}\tilde{\zeta} + (1/2)\partial^2 p_{sh}/\partial\zeta^2|_{\varepsilon_F}\tilde{\zeta}^2 + ..., \tag{13}$$

and retaining only terms of the first order in $\tilde{\zeta}$ we can define the equation for chemical potential oscillations in the guise represented by the equation (9) with fundamental frequency,

$$F = \frac{\varepsilon_F}{\mu_c} = \frac{p_{sh}(\varepsilon_F)}{A}, \tag{14}$$

where the last equality represents the equation for Fermi energy ε_F.

Concentration of holes in 1D subband can be represented as:

$$p_{sh}(\zeta) = \frac{1}{v\sqrt{\varepsilon_{sh}}} \int_0^\infty (1 + \exp[(\zeta - \Delta + \varepsilon)\beta])^{-1} \frac{d\varepsilon}{\sqrt{\varepsilon}}, \tag{15}$$

where $\varepsilon_{sh} \equiv \hbar(\pi/b)^2/2|m_{sh}|$, $m_{sh} < 0$ is the negative effective mass of electrons moving on hole-like open orbits inside the 1D Fermi surface sheet (see Fig. 2) with dispersion law $\varepsilon_{\mathbf{k}} = \Delta - \hbar^2(\pi/b - k)^2/2|m_{sh}|$, $k \equiv k_y$ is the wave vector component along the direction perpendicular to the planar Fermi surface 1D sheet (dispersion along sheet is neglected), $v = abc^*$ is the unit cell volume, a and b are the lattice constants in the k_x- and k_y-directions. In a case of degeneracy of holes, $(\Delta - \zeta) \gg k_B T$, we obtain:

$$p_{sh}(\zeta) \cong \frac{1}{v\sqrt{\varepsilon_{sh}}}(\Delta - \zeta)^{1/2}. \tag{16}$$

In the latter case we get from the equation (14) the equation for determination of the Fermi energy

$$\varepsilon_F = \varepsilon_{ef}^{1/2}(\Delta - \varepsilon_F)^{1/2}, \qquad \varepsilon_{ef} \equiv 2\frac{|m_{sh}|}{m_{c0}}\frac{\hbar^2 a^{-2}}{m_{c0}}, \tag{17}$$

with solution:

$$\varepsilon_F = (\varepsilon_{ef}/2)(\sqrt{1 + 4\Delta/\varepsilon_{ef}} - 1). \tag{18}$$

For transfer parameter, equation (11), we obtain for the case of degenerate holes (see Eq. (16)):

$$c_R^{(ov)} = \frac{\varepsilon_{ef}^{1/2}}{2(\Delta - \varepsilon_F)^{1/2}} = \frac{\varepsilon_{ef}}{2\varepsilon_F} = \frac{1}{2(\Delta/\varepsilon_F - 1)} = \frac{1}{\sqrt{1 + 4\Delta/\varepsilon_{ef}} - 1}. \tag{19}$$

Let us calculate the transfer parameter for 2D organic metal α-$(ET)_2KHg(SNC)_4$ supposing that situation with hole pocket + electron sheet gives the same results for transfer parameter as electron pocket + hole sheet. Using the calculations of its band structure in reference [2,27] from where we can obtain $\Delta/\varepsilon_F \cong 1.5$ and using relation $\Delta/\varepsilon_{ef} = \Delta/\varepsilon_F(\Delta/\varepsilon_F - 1)$ (following from the Eq. (17)) we obtain $\Delta/\varepsilon_{ef} \cong 0.75$ and $c_R^{(ov)} \cong 1$.

Proportionality relation between magnetization and chemical potential oscillations in a 2D metal under high quantizing magnetic field has been recovered for ensemble of electrons filling spin-degenerate discrete energy levels [18] (spin-degenerate Landau levels). The total number of electrons on corresponding quantized closed orbits was supposed to be constant (independent on magnetic field). Similar relation has been proved for such an ensemble in the presence of reservoir of electrons situated on magnetic field independent levels [17]. Acting as in reference [17] (see Appendix) we obtain for 2D electron system with spin-split Landau levels (at temperatures and magnetic

fields fulfilling the conditions: $k_{\rm B}T \lesssim \hbar\omega_{\rm c}(B)$ ($Q \gtrsim 1$) and $B/F = \hbar\omega_{\rm c}(B)/\varepsilon_F \ll 1$) the same relation as for the case of spin-degenerate quantum levels (more exactly, as for the case with electron g-factor $g \equiv 0$):

$$\frac{M(b)}{M_0} = \frac{2}{\hbar\omega_{\rm c}(B_{\bar n})}(1+c_{\rm R})\tilde\zeta(b). \qquad (20)$$

Both this relation and equation for the chemical potential oscillations (Eq. (9)) provide the framework inside which *the complete picture of magnetization oscillations may be described quantitatively: not only the oscillations amplitudes but also their wave forms may be calculated for any strength of electrons transfer between quantum (field dependent) and field independent energy levels.* The knowledge of oscillations wave forms may be of interest in problems connected with magnetic interaction [1] of electrons leading to effects of magnetic instability inside Fermi liquid: diamagnetic phase transitions and diamagnetic (Condon) domains [28].

3 Wave form of spin-split chemical potential and magnetization oscillations. Comparison to experiment

Here we generalize the parametric method, derived in reference [17] for spin-degenerate levels, for calculation of wave forms of the chemical potential and magnetization oscillations with spin-split structure. Throughout this chapter we will not identify the definite reservoir determining the value of the transfer parameter $c_{\rm R}$, hence, the results will be valid for any reservoir.

Extending the separated level $\varepsilon_{\bar n,-1}(B)$ in a series on small quantity $b/B_{\bar n}$:

$$\varepsilon_{\bar n,-1}(B) = \varepsilon_{\bar n,-1}(B_{\bar n}) + \left.\frac{\partial\varepsilon_{\bar n,-1}}{\partial B}\right|_{B_{\bar n}}(B-B_{\bar n}) + \cdots$$
$$= \varepsilon_{\rm F} + (1-s)\frac{\hbar\omega(B_{\bar n})}{2} + \frac{\varepsilon_{\bar n,-1}(B_{\bar n})}{B_{\bar n}}b + \cdots, \qquad (21)$$

and presenting the chemical potential as: $\zeta(B) = \varepsilon_{\rm F} + \tilde\zeta(b)$ we obtain the variable $x = [\varepsilon_{\bar n,-1}(B) - \zeta(B)]/k_{\rm B}T$ by using the condition $2b_{\bar n} \ll B_{\bar n}$ in the form:

$$\frac{2}{Q}x = 1 - s + \frac{b}{b_{\bar n}} - \frac{2}{\hbar\omega_{\rm c}}\tilde\zeta(b), \qquad (22)$$

where $b_{\bar n}$, determined here as $2\varepsilon_{\bar n,-1}(B_{\bar n})/\hbar\omega_{\rm c}(B_{\bar n})B_{\bar n} \cong 2\varepsilon_{\rm F}/\mu_{\rm c}B_{\bar n}B_{\bar n} = 2F/B_{\bar n}B_{\bar n} \cong 2F/B_{\bar n+1}B_{\bar n} = 1/b_{\bar n}$, coincide with the earlier definition of the halfperiod in the approximation, $2b_{\bar n}/B_{\bar n} \ll 1$. Exact definition of the quasiperiod is (see Fig. 1): $2b_{\bar n} = B_{\bar n} - B_{\bar n+1} \equiv B_{\bar n,\bar m-1} - B_{\bar n+1,\bar m} = B_{\bar n+1,\bar m}B_{\bar n,\bar m-1}/F \equiv B_{\bar n+1}B_{\bar n}/F$. This follows from the relations: $F = B_{\bar n,\bar m-1}(\bar n+\bar m)/2 = B_{\bar n+1,\bar m}(\bar n+1+\bar m+1)/2 = B_{\bar n,\bar m}(\bar n+\bar m+1)/2$ corresponding to magnetic fields at the right end of the period, at the left end and in the center (these relations follow from definitions of those magnetic fields corresponding to intersections of mean curves between spin-split levels with the Fermi level in the singled period, Eqs. (4) and (5)). Note the identity definitions used throughout: $B_{\bar n,\bar m-1} \equiv B_{\bar n}$ and $B_{\bar n+1,\bar m} \equiv B_{\bar n+1}$ and $B_{\bar n,\bar m} \equiv \bar B_{\bar n}$, see Figure 1. In the above derivation of the equation (22) we have ignored the field dependence of the separation between levels with the same spin, *i.e.* of $\hbar\omega_{\rm c}(B)$, within the singled quasiperiod. The account of this dependence reveals the asymmetry of the oscillations inside any quasiperiod. The following expressions obtained within first order in the approximation $2b_{\bar n} \ll B_{\bar n}$ will give antisymmetric wave form inside any period.

Solving the pair of equations, equations (9) and (22), relative to the variables $\tilde\zeta$ and $b/b_{\bar n}$ we obtain them as explicit functions of x, which will be served here as a parametric variable:

$$\frac{2}{\hbar\omega_{\rm c}}\tilde\zeta(x) = \frac{1}{1+c_{\rm R}}\left[-2g_{\rm s}(x,Q) + \left(1-s-\frac{2}{Q}x\right)\right], \qquad (23)$$

$$-\frac{b(x)}{b_{\bar n}} \equiv -\frac{k_{\bar n}b(x)}{\pi} = \frac{2}{1+c_{\rm R}}\left[g_{\rm s}(x,Q) + \frac{c_{\rm R}}{2}\left(1-s-\frac{2}{Q}x\right)\right]. \qquad (24)$$

Changing the parametric variable x in the interval corresponding to the separated fixed period ("boundary" conditions for the parametric variable x, see Fig. 1):

$$-(1+s)\frac{Q}{2} \leqslant x \leqslant (1-s)\frac{Q}{2}, \qquad (25)$$

we obtain explicit solution for the chemical potential oscillations as a function of magnetic field, $\tilde\zeta(b)$, in the separated quasiperiod $-2b_{\bar n} \leqslant b \leqslant 0$ (see the left period relative to the fixed magnetic field $B_{\bar n}$ in Fig. 1). It should be noted that due to the spin-splitting the "boundary" conditions for the parametric variable at the ends of a singled period are asymmetrical (contrary to the case of $s = 0$ where they are antisymmetric: $-Q/2 \leqslant x \leqslant Q/2$).

As it is seen from equations (23) and (24) and "boundary" conditions for the separated period (Eq. (25)) the parametric solution for the chemical potential oscillations in a case of spin-split levels is determined by the three parameters: the temperature smoothing parameter Q, characterizing magnetic field and temperature, the spin-splitting parameter s, characterizing the electron g-factor, and the transfer parameter $c_{\rm R}$, describing the thermal exchange of carriers between Fermi surface cylinder and open parts of the Fermi surface and/or localized states. As it is seen, namely this latter parameter influences the amplitude of the chemical potential oscillations suppressing it greatly at all Q: from equation (23) follows that at $c_{\rm R} \gg 1$ the oscillating part of the chemical potential $\tilde\zeta \to 0$ at all magnetic fields inside the period, $-2b_{\bar n} \leqslant b \leqslant 0$ (note that the $g_{\rm s}(x,Q)$ function changes in the range $0 \leqslant g_{\rm s}(x,Q) \leqslant 1$ and as was shown in Ref. [11] the maximal value of the parametric variable x is $x_{\rm m} \cong \ln[(Q/2)(1+\exp(-sQ))]$, both independent on the transfer parameter $c_{\rm R}$).

The parametric method allows in calculation of the g_s-function to sum on constraint number (usually a few) of symmetrical pairs of electron-like and hole-like levels around the Fermi level. This is the essence of the approach which we call the level approach (in contrast to the Lifshitz-Kosevich (LK) approach which may be called the harmonic approach). The LK harmonic approach based on the Poisson summation formula is better justified and more simple for application in low magnetic field-high temperature region ($Q \lesssim 10$). The level approach works better in the high magnetic field-low temperature region ($Q \gtrsim 10$). As will be shown later on except for the high temperature-low magnetic field region ($Q < 5$) leaving only one term in sums entering into the g_s-function is enough for getting the exact results. In this approach only six spin-split levels around the Fermi level are taken into account (six spin-split level approximation, see Fig. 1) which gives exact results for all actual region of temperatures and magnetic fields ($Q \gtrsim 5$) and all values of spin-splitting parameter, $0 \leqslant s \leqslant 0.5$. On taking into account the antisymmetry of magnetization inside any period the necessary number of spin-split levels reduces to three. *The merit of parametric method that it gives the exact description not only of the temperature and magnetic field dependences of the amplitudes but also of the wave form of magnetoquantum oscillations.* Parametric method is applicable at all temperatures and magnetic fields under study ($Q \gtrsim 1$) and fully takes into account chemical potential oscillations which are determined by the strength of the equilibrium transfer of carriers between closed orbits and reservoir.

Chemical potential oscillations with spin-split structure for various transfer parameter, c_R, are shown in Figure 1. It is seen that yet at $c_R \sim 1$ (Fig. 1, curve 2) the wave form of the chemical potential oscillations is symmetrized and for large $c_R \gtrsim 10$ (Fig. 1, curve 3) their amplitudes are almost completely suppressed. Hence, in the presence of open parts of the Fermi surface and/or localized states (*i.e.*, for possibility of thermal exchange of quantized carriers with nonquantized ones from reservoir) for moderate values of the transfer parameter $c_R \sim 1$ the chemical potential oscillations are seen as symmetric even at ultralow temperatures, $T \to 0$. In low temperature-high magnetic field region (for large Q beginning from $Q \gtrsim 10$) the oscillations of the chemical potential have nearly sawtooth shape for small transfer parameter $c_R \ll 1$ (this is relevant also for spin-split structure at $sQ \gtrsim 10$ (see Fig. 1, curve 1)).

The expression for the chemical potential (Eq. (23)), being substituted into the expression for the magnetization, equation (20), gives magnetization as a function of parametric variable x:

$$\frac{M(x)}{M_0} = 1 - s - 2g_s(x, Q) - \frac{2}{Q}x. \tag{26}$$

Taking derivative with respect to b of the equation (26) and noting that $(\partial x/\partial b)_{b_{ex}} = Q/2b_{\bar{n}}$ (see Eq. (22)) we obtain at the extremums of magnetization (or chemical potential) the equation for the corresponding value of parametric variable, $x_{ex} \equiv x(b_{ex})$:

$$\frac{1}{Q} = -\frac{\partial g_s(x, Q)}{\partial x}\Big|_{x_{ex}}. \tag{27}$$

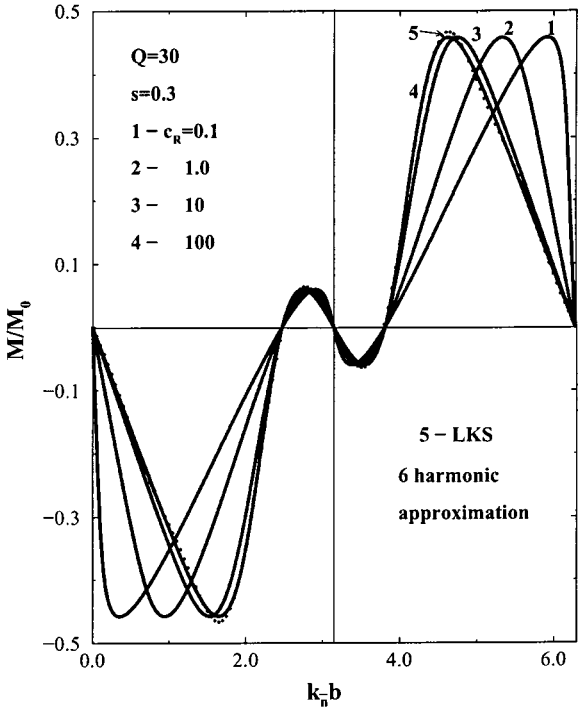

Fig. 3. Spin-split magnetization oscillations in 2D metal in the intermediate temperature-magnetic field region: $Q = 30$. Calculated in level approach according to the parametric equations (24–26) with g_s-function (Eq. (10)) taken in 6 spin-split level approximation. Spin-splitting parameter is $s = 0.3$. Curves 1–4 are drawn for different transfer parameter $c_R = 0.1, 1.0, 10, 100$. Curve 5 (dotted) is plotted according to LKS formula (see Eq. (28)) taken in 6 harmonic approximation. Note shifting of the main and spin-splitting maxima to the left and symmetrizing of the wave shapes of oscillations with increasing transfer parameter c_R. Note also the coincidence of shapes in harmonic (curve 5) and level (curve 4) approaches for large transfer parameter $c_R = 100$.

Remarkable, that the values of the parametric variable, x_{ex}, corresponding to the magnetic fields where the extremums of the magnetization (and chemical potential) take place, b_{ex}, are found from the last equation, which is independent on the transfer parameter, c_R. We see that *the magnetization amplitudes* $M(x_{ex})$ (the main (Mn) and that of the spin-split structure (ss) [11]) obtained from equation (26) *are also independent on the transfer parameter.* The connection between b_{ex} and x_{ex} is through the equation (24) dependent on the transfer parameter. Consequently, *magnetic fields of the extremal values of magnetization,* b_{ex}*, determining the wave form of oscillations, are greatly depending on the transfer parameter,* c_R.

These results are illustrated in Figures 3 and 4 for low and ultralow temperatures. Magnetization oscillations

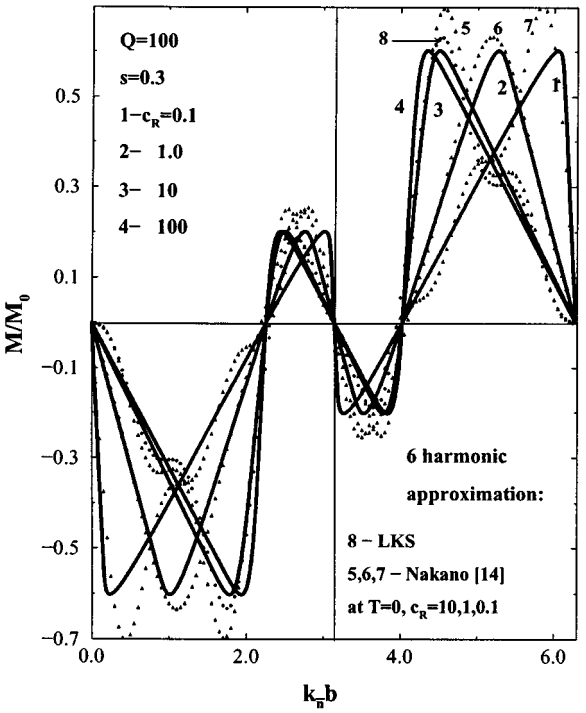

Fig. 4. Spin-split magnetization oscillations in 2D metal in ultralow temperature-high magnetic field region: $Q = 100$. Calculations as in Figure 3. Note the triangle shape of oscillations in the level approach (curves 1–4) and additive structure on the right side of the main maximum in harmonic approach (dotted curve 8) which may be due to the insufficiency of the 6 harmonic approximation in the LKS formula for description of wave form at such low temperature. Curves 5, 6 and 7 (triangle symbols) correspond to spin-split oscillations at $T = 0$, $s = 0.3$ and transfer parameter $c_{\rm R} = 10, 1.0, 0.1$ (calculated according to formulae obtained in harmonic approach with explicit account of background (unquantized) states in the Ref. [14], see text, Sect. 3). Note also the additive structure on curves 5 ($c_{\rm R} = 10$) and 7 ($c_{\rm R} = 0.1$) as on the LKS curve 8.

with spin-split structure are seen as smooth in intermediate temperature-magnetic field region (which may be defined approximately as determined by the values of the Q-parameter and spin-splitting parameter, $sQ \gtrsim 10$, Fig. 3), and of the triangle-like shape in the ultralow temperature-high magnetic field region ($sQ \gtrsim 30$, Fig. 4). For values of the transfer parameter $c_{\rm R} \sim 1$ the oscillations are seen as symmetric as compared with sawtooth-like shape at $c_{\rm R} \ll 1$ and inverse-sawtooth-like shape at $c_{\rm R} \gg 1$. It is interesting to note that for the value of the transfer parameter to be equal to unity, $c_{\rm R} = 1$, magnetization oscillations are seen as strictly symmetrical at ultralow temperatures, $T \to 0$ (compare curves 2 from Figs. 3 and 4). This result was rigorously obtained in reference [18] for spin-unsplit ($s = 0$) oscillations *via* calculation of paramagnetic, $\chi_{\rm p}$, and diamagnetic, $\chi_{\rm d}$, susceptibilities at the center and edge of the period (at magnetic fields $\bar{B}_{\bar{n}}$ and $B_{\bar{n}}$ (see Fig. 1)): it was shown that $|\chi_{\rm d}|/\chi_{\rm p} \to 1/c_{\rm R}$ at $T \to 0$. For comparison with our results it is useful to represent the LK formula (LK formula adapted for 2D systems by Shoenberg [23] – LKS formula) as a series of harmonics, functions of magnetic field counted from the fixed magnetic field, $B_{\bar{n}}$ ($b = B - B_{\bar{n}}$):

$$M^{(\rm LKS)}(b)/M_0 = \sum_{l=1}(-1)^l a_l(s,Q)\sin(lk_{\bar{n}}b), \qquad (28)$$

where $a_l(s,Q) = 4\pi\cos(l\pi s)/[Q\sinh(l2\pi^2/Q)]$ are the amplitudes of harmonics for spin-split levels [1]. This formula serves for even numbers of the integer parameter $I = [G]$, for odd numbers of I the factor $(-1)^l$ should be omitted and the above formula describes oscillations shifted on half period. Magnetization oscillations with spin-split structure calculated according to the LKS formula, equation (28), are shown in Figure 3 (curve 5) and Figure 4 (curve 8) (dotted curves). As expected they nearly coincide with exact results obtained in the level approach (Eqs. (24–26)) for large transfer parameter $c_{\rm R} \gtrsim 10$. We see that at substantial values of the transfer parameter $c_{\rm R} \gg 1$ the main and spin-split maximums shift to the left, on very great values reaching those positions obtained by the LKS formula. It is clear now, *why the LK-type formulae neglecting completely the chemical potential oscillations in 2D metals have been such successfully used for determining the cyclotron mass from the temperature dependence of magnetization oscillations amplitudes. The answer is clear from the above results: because of the independence of magnetization amplitudes on chemical potential oscillations.*

Recently the spin factor of de Haas-van Alphen oscillations in the model of 2D quantized + 2D unquantized bands (2D unquantized band serving as the electron reservoir) at $T = 0$ was obtained in the formalism of harmonic approach [14]. The analytical formula for magnetization as function of magnetic field can be represented as $M^{(Nak)}/M_0 = (2/\pi)\Sigma_{l=1}[(-1)^l/l]R_l(s,c_{\rm R})\sin(lk_{\bar{n}}b)$ (where the spin-factor $R_l(s,c_{\rm R})$ should be taken from the Ref. [14]) and in this form compared with our results at ultralow temperature (see Fig. 4, curves 5–7).

The explicit solution for magnetization with spin-split structure can be provided only in the case of completely fixed chemical potential (at $c_{\rm R} \to \infty$) inside any period, $-2b_{\bar{n}} \leqslant b \leqslant 0$:

$$\frac{M(b)}{M_0} = -\frac{b}{b_{\bar{n}}} - 2g_{\rm s}(x,Q), \qquad x(b) = \frac{Q}{2}\Big(1 - s + \frac{b}{b_{\bar{n}}}\Big), \qquad (29)$$

which serves as the level approach analog of the harmonic approach given by the LKS formula (28).

For the span between main and spin-split maxima we obtain using equation (27):

$$\frac{w}{2b_{\bar{n}}} \cong 1 - \frac{1}{1+c_{\rm R}}\Big[\frac{1}{2} + c_{\rm R}(1-s)\Big]. \qquad (30)$$

The above simple relation can be used for estimating the spin-split parameter s if transfer parameter $c_{\rm R}$ is known or *vice versa* for given experimental value of $w/2b_{\bar{n}}$. For constant number of quantized carriers ($c_{\rm R} = 0$) the span

between magnetic fields corresponding to the minimal (maximal) values of magnetization is $w/2b_{\bar{n}} = 1/2$, *i.e.* equal to the halfperiod. For constant chemical potential ($c_{\rm R} \to \infty$) we have $w/2b_{\bar{n}} = s$. For $c_{\rm R} = 1$ the span $w/2b_{\bar{n}} = 1/4 + s/2$, *i.e.* for $s \lesssim 0.5$ is slightly less than halfperiod.

Let us compare our analytical results concerning wave forms of magnetization oscillations with spin-split structure with available experimental data for quasi-two-dimensional organic metal α-$(ET)_2KHg(SNC)_4$ (and the like salts). This substance is known to undergo the phase transition around the so called kink magnetic field $B_{\rm K} \simeq 23$ T with changing of the cyclotron mass from value under (un) kink field $m_{\rm c}^{(\rm un)}/m_{\rm e} = 1.5$ to the value above (ab) $m_{\rm c}^{(\rm ab)}/m_{\rm e} = 1.65$ (see Ref. [6]) and the $gm_{\rm c}/m_{\rm e} \equiv 2G$ value from $2G^{(\rm un)} = 4.7$ (which corresponds to spin-splitting parameter $s^{(\rm un)} = 0.35$, see Eq. (6)) to $2G^{(\rm ab)} = 3.63$ ($s^{(\rm ab)} = 0.185$) (for the experimental $gm_{\rm c}/m_{\rm e} \equiv 2G$ values in phases under and above kink field, see Ref. [8]). There is not up to now an unanimous opinion about Fermi surface structure of this salt under the kink field at low temperatures where the prominent split structure in magnetization is observed [3]. There are various calculations of their band structure (see reviews [2,3]) admitting the different nesting of the quasi-1D Fermi surface sheets and, consequently, the reconstructed Fermi surface [29]. Nevertheless, we will risk to explain the attenuation of the amplitude of the split magnetization under the kink field by the spin-splitting effect (see also another explanation in Ref. [30] as due to the effect of frequency doubling). The spin-split structure is revealed in experiment at rather low temperature under the kink field and disappears above [6]. This effect is confirmed by our analytical results shown in Figures 5a (at $B = 20$ T) and Figure 5b (at $B = 25$ T). The behavior of spin-split structure in two phases may be explained by the combined changes in cyclotron mass (changes in temperature smoothing Q-parameter) and the g-factor (changes in spin-splitting s-parameter). The wave form (*i.e.* shift of the maximum to the symmetrical position) is being determined by the influence of open parts of the Fermi surface and/or localized states (the transfer parameter, calculated for the unreconstructed Fermi surface of the abovementioned material is $c_{\rm R}^{(\rm ov)} \cong 1$). Note that even in the model of reconstructed Fermi surface the electron reservoir of background unquantized states might be remained, in this case being due to the sections of unquantized bands of one or two dimensionality (the transfer parameter for model of spin-split 2D quantized + 2D unquantized bands at $T = 0$ was considered recently in the Ref. [14]). We see from Figure 5b that the calculated spin-split structure above kink field disappears entirely at slightly decreased spin-splitting parameter than that obtained experimentally in reference [8]. This discrepancy may be due to the influence of level broadening which may also suppress spin-splitting structure even at higher values of spin-splitting parameter. The level broadening due to impurity scattering has been accounted for recently in references [31,32] for models with fixed chemical potential ($c_{\rm R} \to \infty$) and constant number of electrons on quantized levels ($c_{\rm R} = 0$). The theory of magnetization oscillations in framework of level approach accounting for broadened spin-split Landau levels and any background density of states ($\infty > c_{\rm R} > 0$) is in progress.

4 Conclusion

The paper is devoted to the development of a theory of magnetoquantum oscillations with spin-split structure in a 2D metal in the framework of formalism of level approach – direct summation on quantum levels around Fermi level in any period of oscillations [12,18,26]. Parametric method [17] was generalized for getting wave forms of spin-split oscillations. Equilibrium exchange of carriers between spin-split levels and field independent levels represented by the reservoir *via* equation for chemical potential oscillations accounts for the diversity of wave forms of spin-split magnetization oscillations. The effect of spin-splitting has been unaccounted for in the previous models which did take into account chemical potential oscillations [18,33], but dealt with spin-degenerate (unsplit) energy levels.

Analytical parametric formulae for calculating wave forms of spin-split oscillations are expressed *via* the $g_{\rm s}$-function containing summation on pairs of spin-split electron and hole levels symmetric inside the given period. The simplicity of the formalism of level approach manifests itself in calculations when only a few number of levels should be taken into account in all actual region of magnetic fields and temperatures and spin-splitting parameter. In extreme case of ultra-low temperatures ($Q \gg 10$), in a model with spin-split levels, for calculating of the main and spin-split amplitudes only account of two spin-split separated in singled period levels is enough [11]. Exact wave form of oscillations is obtained here by using only six spin-split levels (see Fig. 1) in all actual region of temperature-magnetic field (for all values of the temperature smoothing parameter $Q \gtrsim 5$ and in all region of spin-splitting parameter $0 \leqslant s \leqslant 0.5$). If we take into account that for periods corresponding to large quantum numbers the magnetization is antisymmetric function relative to the center of period the needed spin-split levels are reduced to three. The merit of the level approach that it fully employs the inherent local symmetry of level dispositions relative to the Fermi energy inside any period.

We have proved general proportionality relation between magnetization and chemical potential oscillations [17] for system with quantum spin-split levels and magnetic field independent states. Main amplitude, so as spin-split amplitude [11], are proved to be independent on the presence of electron reservoir. All the difference for models of intersecting or overlapping 2D and 1D bands is in the concrete expression for the transfer parameter $c_{\rm R}$ entering in general form into the basic equation for chemical potential oscillations (Eq. (9)), which in its turn is written in its canonical form with $g_{\rm s}(x, Q)$-function (Eq. (10)). Here we have calculated the corresponding deposition $c_{\rm R}^{(\rm ov)}$ into the transfer parameter $c_{\rm R}$ in the model

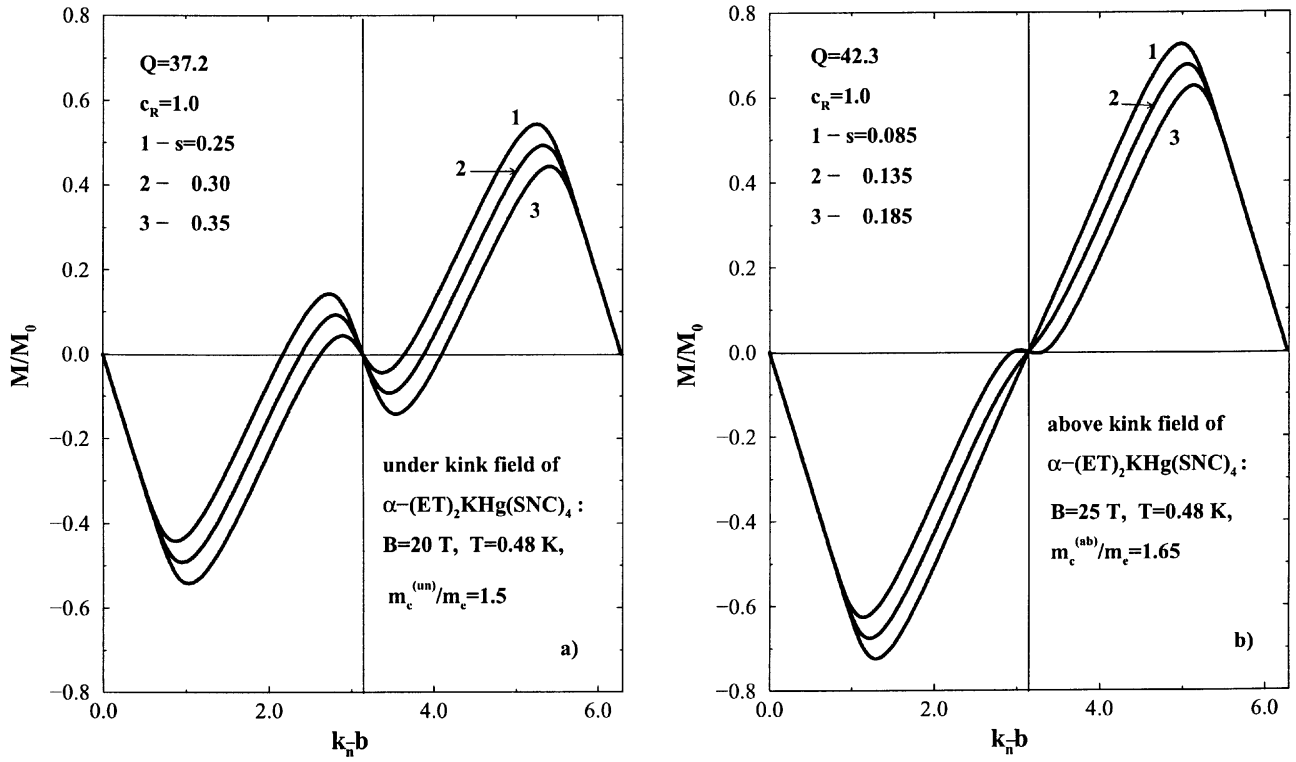

Fig. 5. Magnetization oscillations around kink magnetic field $B_{\rm K} \cong 23$ T in organic metal α-$(ET)_2KHg(SNC)_4$ (calculated according to the Eqs. (24–26) with $g_s(x,Q)$-function, Eq. (10), taken in 6 spin-split level approximation). (a) under kink field: $B = 20$ T, $T = 0.48$ K, $m_c^{(un)}/m_e = 1.5$ (experimental data from Ref. [6], corresponding parameter $Q = 37.2$). Spin-splitting parameter $s^{(un)} = 0.35$ corresponds to the experimental value $(gm_c/m_e)^{(un)} = 4.7$ obtained in the reference [8]. Note that spin-split structure under kink field persists at all values of spin-splitting parameter used: curve 1: $s = 0.25$, curve 2: $s = 0.30$, curve 3: $s = 0.35$. (b) above kink field: $B = 25$ T, $T = 0,48$ K, $m_c^{(ab)}/m_e = 1.65$ (experimental data from Ref. [6], corresponding parameter $Q = 42.3$). Spin-splitting parameter above kink field $s^{(ab)} = 0.185$ corresponds to the experimental value of $(gm_c/m_e)^{(ab)} = 3.63$ from reference [8]. Note that slight hint on the spin-split structure above kink field for spin-splitting parameter $s = 0.185$ (curve 3) disappears at $s = 0.135$ (curve 2) and $s = 0.085$ (curve 1). Note that all calculated curves from (a) and curves 2 and 1 from (b) repeat obtained in reference [6] experimental structure of magnetization oscillations around kink field (KF): with spin-split structure under KF and without above.

of overlapping 2D and 1D bands characteristic of quasi 2D organic metals.

The wave form of spin-split oscillations obtained at low and ultralow temperatures differs distinctly. At low temperatures ($sQ \gtrsim 10$) the shape of magnetization oscillations is seen as rather smooth. At ultralow temperatures the wave form of oscillations acquires the triangle-like shape. At transfer parameter $c_{\rm R} = 1$ and ultralow temperature, $T \to 0$, the oscillations are looking as completely symmetrical. This contrasts distinctly the extreme cases of constant number of quantized carriers ($c_{\rm R} = 0$) and constant chemical potential ($c_{\rm R} \to \infty$) for which magnetization oscillations acquire extreme sawtooth (with maximums shifted to the extreme right) and inverse sawtooth (with maximums shifted to the extreme left) wave forms correspondingly.

As example of application of the developed theory accounting for the spin-splitting effect in Landau levels we compare calculated magnetization oscillations wave forms at magnetic fields around kink magnetic field in organic metal α-$(ET)_2KHg(SNC)_4$. For given experimental parameters (see Ref. [3,6]) our theory confirms the presence of spin-split structure at magnetic fields under the kink field and the absence above, which is an experimental yield connected with difference in the corresponding gm_c/m_e value [8] (and consequently, in values of spin-splitting parameter s) in both phases. We have calculated the transfer parameter for model of overlapping bands that can describe the possible situation in the abovementioned metal and obtained according to the calculated value, $c_{\rm R}^{(ov)} \cong 1$, *symmetrical wave forms of magnetization oscillations* both with spin-split structure and without it *notwithstanding the relatively high temperature smoothing parameter* Q. Our comparison hints on the prevailing role of the change in the g-factor rather than the cyclotron mass in traversing the phase transition around

$$\frac{\Omega_{\rm LL}(B,\zeta)/V}{A} = -\frac{B}{\beta}\Bigg[\sum_{n=0}^{\bar{n}-1}\frac{1}{2}(\zeta-\varepsilon_{n,-1})\beta+\frac{1}{2}\ln\left(1+\exp[(\zeta-\varepsilon_{\bar{n},-1})\beta]\right)+\sum_{m=0}^{\bar{m}-1}\frac{1}{2}(\zeta-\varepsilon_{m,1})\beta+\frac{1}{2}\ln\left(1+\exp[(\zeta-\varepsilon_{\bar{m},1})\beta]\right)$$
$$+\sum_{n=0}^{\bar{n}-1}\frac{1}{2}\ln(1+\exp[(\varepsilon_{n,-1}-\zeta)\beta])+\sum_{n=\bar{n}+1}\frac{1}{2}\ln(1+\exp[(\zeta-\varepsilon_{n,-1})\beta])$$
$$+\sum_{m=0}^{\bar{m}-1}\frac{1}{2}\ln(1+\exp[(\varepsilon_{m,1}-\zeta)\beta])+\sum_{m=\bar{m}+1}\frac{1}{2}\ln(1+\exp[(\zeta-\varepsilon_{m,1})\beta])\Bigg]. \quad \text{(A.1)}$$

kink field. It should be noted that our explanation of the split structure of magnetization under kink field is one of the possible because topology of the Fermi surface in α-$(ET)_2KHg(SNC)_4$ and the like salts is the subject for further study [3] (see also Ref. [30] where the effect of frequency doubling as cause of the split oscillations under the kink field is proposed).

Calculation of wave forms of magnetoquantum oscillations with spin-split structure in frameworks of exactly soluble models as has been done in the present work will be useful in establishing electronic structure of 2D metals (organic and those having quasicylindrical parts of Fermi surface) with account of spin-splitting effect. The experiments with high resolution of magnetoquantum oscillations spectra, including their shape on the length of period of oscillations, will be basic checking tool proving the validity of employed analytical models.

Valuable discussions with T. Maniv, I.D. Vagner and J. Wosnitza are greatly appreciated. The support of the Center for Absorption in Science, Ministry of Immigrant Absorption, State of Israel (KAMEA Foundation), and the Israel Science Foundation (Israel Academy of Sciences and Humanities) is acknowledged.

Appendix A: Proportionality relation between magnetization and chemical potential oscillations in a 2D electron system with spin-split Landau levels and background reservoir states

Here we provide derivation of the basic equation for the chemical potential oscillations and proportionality relation for magnetization in a 2D metal in the model of intersecting 2D and 1D bands, the electrons of the 2D subband filling spin-split Landau levels and those of a 1D band filling the magnetically unperturbed reservoir states. Model of intersecting bands but not accounting for spin-splitting effect was considered in reference [17]. The analysis that will be undertaken may be called the formalism of level approach [11,12,18,26] (in contrast to the harmonic approach represented by the LK-type formulae based on the Poisson summation formulae (see also [14,16])).

Let us separate two nearest levels with opposite projections of spin (designated by fixed quantum numbers $\bar{n}$ and $\bar{m}$, see Fig. 1), intersecting the Fermi level in a single period. Rearranging summation in the thermodynamic potential (Eq. (1)) on the two sets of spin-split levels with opposite projections of spin lying under and above of separated levels (levels in each set are symmetric relative to the corresponding separated level in the singled period (see Fig. 1)) we have:

see equation (A.1) above.

In the above representation we have separated the independent implicitly on temperature the main deposition to the thermodynamic potential of the completely filled levels under the Fermi level (with quantum numbers $n<\bar{n}$ and $m<\bar{m}$), the deposition of the levels intersecting the Fermi level, $\varepsilon_{\bar{n},-1}$ and $\varepsilon_{\bar{m},1}$, and dependent explicitly on temperature depositions of almost empty electron levels above and almost empty hole levels under the Fermi level.

Note, that in the expressions (1, 4, 5, A.1), we have not so far specified the energy levels, $\varepsilon_{n,-1}(B)$ and $\varepsilon_{m,1}(B)$, except of using their sharpness. In what follows we will use their explicit representation as Landau levels, equations (2) and (3).

Introducing instead of the chemical potential oscillations the dimensionless variable – the energetic difference between the separated level $\varepsilon_{\bar{n},-1}(B)$ and the chemical potential $\zeta(B,T)$ in $k_{\rm B}T$ units (see Fig. 1):

$$x(B,T)\equiv[\varepsilon_{\bar{n},-1}(B)-\zeta(B,T)]\beta, \quad \text{(A.2)}$$

and temperature smoothing parameter:

$$Q(B,T)\equiv\hbar\omega_{\rm c}\beta, \quad \text{(A.3)}$$

we reveal further on the main dependence of the thermodynamic potential on magnetic field in the separated period *via* the nearest energy levels around the Fermi level (see Fig. 1).

The levels crossing the Fermi level inside the separated period (crossing levels), $\varepsilon_{\bar{n},-1}$, $\varepsilon_{\bar{m},1}$, and the almost empty electron and hole energy levels around the Fermi level inside the separated period play the leading role in the temperature dependence of the chemical potential and magnetization oscillations. Filled levels under the Fermi level (the first and third term in the Eq. (A.1)) and the crossing levels determine the main magnetic field dependence

$$\begin{aligned}
\frac{(\Omega_{\rm LL}/V)}{A} &= -\frac{B}{\beta}\Bigg[\sum_{n=0}^{\bar{n}-1}\frac{1}{2}(\zeta-\varepsilon_{n,-1})\beta+\sum_{m=0}^{\bar{m}-1}\frac{1}{2}(\zeta-\varepsilon_{m,1})\beta+\frac{1}{2}\ln\left[1+\exp\left(-x\right)\right]+\frac{1}{2}\ln(1+\exp[-(x+sQ)])\\
&\quad+\sum_{k=1}^{\bar{n}}\frac{1}{2}\Big[\ln(1+\exp[-(kQ+x)])+\ln(1+\exp[-(kQ-x)])\Big]\\
&\quad+\sum_{k=1}^{\bar{m}}\frac{1}{2}\Big(\ln\left[1+\exp(-[kQ+(x+sQ)])\right]+\ln\left[1+\exp(-[kQ-(x+sQ)])\right]\Big)\Bigg]\\
&= -B\sum_{n=0}^{\bar{n}-1}\frac{1}{2}(\zeta-\varepsilon_{n,-1})-B\sum_{m=0}^{\bar{m}-1}\frac{1}{2}(\zeta-\varepsilon_{m,1})-\frac{B}{\beta}f_{\rm s}(x,Q),\\
f_{\rm s}(x,Q) &= f_{-1}(x,Q)+f_1(x+sQ,Q),\\
f_{-1}(x,Q) &\equiv \frac{1}{2}\ln\Big[1+\exp\left(-x\right)\Big]+\sum_{k=1}^{\bar{n}}\frac{1}{2}\ln\Big[1+2\exp\left(-kQ\right)\cosh x+\exp\left(-2kQ\right)\Big],\\
f_1(x+sQ,Q) &\equiv \frac{1}{2}\ln(1+\exp[-(x+sQ)])\\
&\quad+\sum_{k=1}^{\bar{m}}\frac{1}{2}\ln\Big[1+2\exp\left(-kQ\right)\cosh\left(x+sQ\right)+\exp\left(-2kQ\right)\Big]. \qquad \text{(A.4)}
\end{aligned}$$

at $T\to 0$. With the above arrangements (Eqs. (A.1–A.3)) we obtain the representation of the thermodynamic potential of quantized carriers:

See equation (A.4) above.

In reality, only a few levels around the Fermi level will play sufficient role in determining the magnetoquantum oscillations. Therefore, in the representation of the thermodynamic potential, equation (A.4), are omitted the depositions of the levels with quantum numbers $n>2\bar{n}$ and $m>2\bar{m}$ as giving negligibly small contributions on large $\bar{n}\gg 1$ and $\bar{m}\gg 1$ relative to the remaining terms described by the symmetrically disposed levels under and above the Fermi level.

Now let us elucidate the deposition into the thermodynamic potential of carriers on magnetic field independent states (nonquantized carriers). Carriers situated around the open parts of the Fermi surface (FS) (regions in the **k**-space inside FS sheets) may fill energy levels which retain continuous spectrum under the high magnetic field. Some carriers may be situated on localized magnetic field independent levels of impurities (defects). The electrons (or holes) on these field independent levels can thermally exchange with carriers on the closed orbits due to the chemical potential oscillations. Spin-splitting of carriers in continuous and localized spectrum being neglected, the thermodynamic potential of the nonquantized carriers is independent explicitly on magnetic field, but only on the chemical potential and does not make the straightforward deposition into the magnetization:

$$\mathbf{M}=-[\partial(\Omega/V)/\partial\mathbf{B}]_\zeta=-[\partial(\Omega_{\rm LL}/V)/\partial\mathbf{B}]_\zeta, \qquad \text{(A.5)}$$

where $\Omega=\Omega_{\rm LL}(B,\zeta)+\Omega_{\rm R}(\zeta)$ is the total thermodynamic potential, $\Omega_{\rm R}(\zeta)$ is the thermodynamic potential of nonquantized carriers representing the reservoir.

Concentration of electrons filling the spin-split levels inside the closed parts of the Fermi surface (here the Fermi surface cylinder – electrons on quantized levels, $n_{\rm LL}$) and reservoir (here the **k**-space inside the open Fermi surface sheets and/or localized states – electrons on nonquantized independent on magnetic field levels, $n_{\rm R}$) is:

$$\begin{aligned}
n_{\rm c} &= -\big(\partial[(\Omega_{\rm LL}(B,\zeta)+\Omega_{\rm R}(\zeta))/V]/\partial\zeta\big)_B\\
&= n_{\rm LL}(B,\zeta)+n_{\rm R}(\zeta), \qquad \text{(A.6)}
\end{aligned}$$

where the total number of electrons, $n_{\rm c}$, is conserved in the magnetic field, $\Omega_{\rm R}(\zeta)=\Omega_{\rm sh}(\zeta)+\Omega_{\rm loc}(\zeta)$ is the thermodynamic potential of electrons filling the reservoir ($\Omega_{\rm sh}(\zeta)$ is the thermodynamic potential of carriers on continuous levels of a FS sheet, $\Omega_{\rm loc}(\zeta)$ is the thermodynamic potential of carriers situated on localized levels). Throughout this appendix we are considering the case of metals with one electron on a unit cell, which in a case of a single not overlapping or not intersecting 2D band provides its half-filling, $n_{\rm c}=1/v$ (v is a unit cell volume).

Let us represent the concentration of nonquantized carriers filling the electron reservoir as a series on the oscillating part of the chemical potential, $\tilde{\zeta}(B,T)=\zeta(B,T)-\varepsilon_{\rm F}$. Taking into account the representation of the thermodynamic potential of quantized carriers, equation (A.4), and retaining only the linear term in the expansion of $n_{\rm R}(\zeta)=n_{\rm R}(\varepsilon_{\rm F}+\tilde{\zeta})$ on $\tilde{\zeta}$, the total concentration of carriers (Eq.(A.6)) may be presented as:

$$\begin{aligned}
n_{\rm c} &= AB\Big[\frac{\bar{n}+\bar{m}}{2}+g_{\rm s}(x,Q)\Big]\\
&\quad+n_{\rm R}(\varepsilon_{\rm F})+[\partial n_{\rm R}(\zeta)/\partial\zeta]_{\varepsilon_{\rm F}}\tilde{\zeta}(B,T), \qquad \text{(A.7)}
\end{aligned}$$

where $g_{\rm s}(x,Q)$-function is determined by the equation (10) in the Section 2.

From the equation (A.7) follows that the fundamental frequency of oscillations relative to the inverse magnetic field, $(1/B)$, can be determined by relations:

$$F=\frac{\varepsilon_{\rm F}}{\mu_{\rm c}}=\frac{n_{\rm c}-n_{\rm R}(\varepsilon_{\rm F})}{A}, \qquad \mu_{\rm c}\equiv\frac{e\hbar}{m_{\rm c}c}\,. \qquad \text{(A.8)}$$

$$\frac{M(B)}{A} = \frac{1}{2}\sum_{n=0}^{\bar{n}-1}\left(\zeta - \varepsilon_{n,-1} - B\frac{\partial\varepsilon_{n,-1}}{\partial B}\right) + \frac{1}{2}\sum_{m=0}^{\bar{m}-1}\left(\zeta - \varepsilon_{m,1} - B\frac{\partial\varepsilon_{m,1}}{\partial B}\right) - B\frac{\partial\varepsilon_{\bar{n},-1}}{\partial B}g_{\rm s}(x,Q) + (1/\beta)f_{\rm s}(x,Q) - \hbar\omega_{\rm c}h_{\rm s}(x,Q),$$

$$h_{\rm s}(x,Q) = h_{-1}(x,Q) + h_1(x+sQ,Q),$$

$$h_{-1}(x,Q) \equiv \frac{1}{2}\sum_{k=1}^{\bar{n}}\frac{k[\cosh x + \exp(-kQ)]}{\cosh x + \cosh(kQ)},$$

$$h_1(x,Q) \equiv \frac{1}{2}\sum_{k=1}^{\bar{m}}\frac{k[\cosh(x+sQ) - s\sinh(x+sQ) + \exp(-kQ)]}{\cosh(x+sQ) + \cosh(kQ)}, \qquad \text{(A.10)}$$

The last equality constitutes equation for determining the Fermi level, $\varepsilon_{\rm F}$, counted from the bottom of the 2D band containing the quantized carriers (see Fig. 2). Note that the fundamental frequency is the same as for the case of degenerate on spin levels.

At magnetic field $B_{\bar{n}}$, as follows from its definition (Eq. (4)), the relation for fixed quantum numbers $\bar{n}$ and $\bar{m}$ holds:

$$\frac{\bar{n}+\bar{m}}{2} = \frac{\varepsilon_F}{\hbar\omega_{\rm c}(B_{\bar{n}})} = \frac{F}{B_{\bar{n}}}, \qquad \text{(A.9)}$$

where in the transition to the last equality the representation $\hbar\omega_{\rm c}(B) = \mu_{\rm c}B$ was used. Taking into account this relation (A.9), we obtain from equations (A.7) and (A.8) the basic equation for the chemical potential oscillations, the equation (9) (see Sect. 2).

Now we will derive in the framework of the considered model of spin-split levels the exact expression for magnetization. Taking the partial derivative of the thermodynamic potential of quantized carriers (in the representation of Eq. (A.4)) with respect to magnetic induction B we obtain the component of magnetization along magnetic field:

see equation (A.10) above,

where the $f_{\rm s}(x,Q)$-function is determined in the equation (A.4). In the sums of these expressions, as in the expression for the chemical potential (Eq. (9) with the $g_{\rm s}$-function from Eq. (10)), we sum on the $\bar{n}$ and $\bar{m}$ pairs of levels under and above the $\varepsilon_{\bar{n},-1}$ and $\varepsilon_{\bar{m},1}$ levels, the above lying levels with quantum numbers $n > 2\bar{n}$ and $m > 2\bar{m}$ being neglected as giving exponentially small depositions into the thermodynamic potential of the order $\exp[-(2\bar{n}+1)Q]$ and $\exp[-(2\bar{m}+1)Q]$ and less for the entire region of $Q \gtrsim 1$. Hence, all the theory is correct for magnetic fields fulfilling the condition: $(\bar{n}+\bar{m})/2 = \varepsilon_{\rm F}/\hbar\omega_{\rm c}(B) \gg 1$.

Performing summation in the first two terms of equation (A.10) on energy levels (Eqs. (2, 3)) lying under the Fermi level we obtain:

$$\frac{1}{2}\sum_{n=0}^{\bar{n}-1}\left(\varepsilon_{n,-1} + B\frac{\partial\varepsilon_{n,-1}}{\partial B}\right) + \frac{1}{2}\sum_{m=0}^{\bar{m}-1}\left(\varepsilon_{m,1} + B\frac{\partial\varepsilon_{m,1}}{\partial B}\right) =$$

$$\sum_{n=0}^{\bar{n}-1}\varepsilon_{n,-1} + \sum_{m=0}^{\bar{m}-1}\varepsilon_{m,1} = \frac{1}{2}(\bar{n}^2+\bar{m}^2)\hbar\omega_{\rm c}(B) - \frac{g}{2}\frac{I}{2}\hbar\omega_{\rm e}(B). \qquad \text{(A.11)}$$

From the equations (A.9) and (8) follows:

$$\frac{1}{2}(\bar{n}^2+\bar{m}^2) = \left[\frac{\varepsilon_{\rm F}}{\hbar\omega_{\rm c}(B_{\bar{n}})}\right]^2 + \left(\frac{I}{2}\right)^2. \qquad \text{(A.12)}$$

The term from the expression for magnetization (A.10), containing the $g_{\rm s}(x,Q)$ function can be written with the help of the equation for the chemical potential, equation (9):

$$-\varepsilon_{\bar{n},-1}(B)g_{\rm s}(x,Q) = \left[\varepsilon_{\rm F} + (1-s)\frac{\hbar\omega_{\rm c}(B_{\bar{n}})}{2}\right]\left[\frac{\varepsilon_{\rm F}}{\hbar\omega_{\rm c}(B_{\bar{n}})}\frac{b}{B_{\bar{n}}} + \frac{c_{\rm R}}{\hbar\omega_{\rm c}(B_{\bar{n}})}\tilde{\zeta}\right]. \qquad \text{(A.13)}$$

In deriving this expression we used the relations: $F/B_{\bar{n}} = (\bar{n}+\bar{m})/2 = \varepsilon_{\rm F}/\hbar\omega_{\rm c}(B_{\bar{n}})$, $\varepsilon_{\bar{n},-1}(B)/B = \varepsilon_{\bar{n},-1}(B_{\bar{n}})/B_{\bar{n}}$ and $\varepsilon_{\bar{n},-1}(B_{\bar{n}}) = \varepsilon_{\rm F} + (1-s)\hbar\omega_{\rm c}(B_{\bar{n}})/2$ (see Fig. 1).

Using the representation $\hbar\omega_{\rm c}(B) = \hbar\omega_{\rm c}(B_{\bar{n}})(1 + b/B_{\bar{n}})$ and substituting the sum on the levels under the Fermi level, equation (A.11) (with Eq (A.12)) and equation (A.13) into the expression (A.10), we obtain for magnetization in the fixed period, $-2b_{\bar{n}} \leqslant b \leqslant 0$:

$$\frac{M(b)}{M_0} = \frac{2}{\hbar\omega_{\rm c}(B_{\bar{n}})}\left\{(1+c_{\rm R})\tilde{\zeta}(b) + \frac{\hbar\omega_{\rm c}(B_{\bar{n}})}{2} \times \left[(1-s)\frac{b}{B_{\bar{n}}} + (1-s)c_{\rm R}\frac{\tilde{\zeta}(b)}{\varepsilon_{\rm F}} + \frac{2k_{\rm B}T}{\varepsilon_{\rm F}}f_{\rm s}(x,Q) - \frac{2\hbar\omega_{\rm c}(B)}{\varepsilon_{\rm F}}h_{\rm s}(x,Q) + \frac{\hbar\omega_{\rm c}(B)}{\varepsilon_{\rm F}}I\left(G - \frac{I}{2}\right)\right]\right\}, \qquad \text{(A.14)}$$

where $M_0 = \varepsilon_{\rm F}\cos\Theta/\phi_0 c^*$ is the saturation magnetization at $T \to 0$.

This is the exact expression for magnetization in the considered model accounting for spin (spin-splitted or spin-nondegenerate Landau levels, the g-factor $g \neq 0$). The first two terms in the square brackets represent the corrections to the oscillating part of magnetization represented by the first term in braces, the last terms in brackets are the steady part of magnetization, the previous to the last term being the diamagnetic contribution (diamagnetism Landau), the last term is the paramagnetic contribution (paramagnetism Pauli). It should be noted that paramagnetic magnetization retains for spin-degenerate quantized levels, *i.e.*, for $s = 0$ (but $G = I \neq 0$).

The oscillating part of magnetization (the first term in braces) contains temperature dependence only through temperature dependence of the chemical potential oscillations and remains finite at $T \to 0$ (as generally $\tilde{\zeta}(b \to 0) \to \hbar\omega_c/2$ at $T \to 0$ (see Fig. 1), while the terms in the brackets will be of the order ($\sim \hbar\omega_c/\varepsilon_F$). Hence, the first term in the braces, proportional to chemical potential oscillations, is the main contribution to the magnetization oscillations (see Eq. (20) of the main text).

References

1. D. Shoenberg, *Magnetic Oscillations in Metals* (Cambridge Univ. Press, Cambridge, 1984).
2. J. Wosnitza, *Fermi surfaces of low-dimensional organic metals and superconductors* (Springer, Berlin, 1996).
3. J. Singleton, Rep. Prog. Phys. **63**, 1111 (2000).
4. J. Wosnitza, G.W. Grabtree, H.H. Wang, U. Geiser, J.M. Williams, K.D. Carlson, Phys. Rev. B **45**, 3018 (1992).
5. T. Sasaki, N. Toyota, Phys. Rev. B **48**, 11457 (1993).
6. S. Uji, J.S. Brooks, M. Chaparala, L. Seger, T. Szabo, M. Tokumoto, N. Kinoshita, T. Kinoshita, Y. Tanaka, H. Anzai, Solid State Commun. **100**, 825 (1996).
7. A.A. House, C.J. Haworth, J.M. Caulfield, S.J. Blundell, M.M. Honold, J. Singleton, W. Hayes, S.M. Hayden, P. Meeson, M. Springford, M. Kurmoo, P. Day, J. Phys. Cond. Matt. **8**, 10361 (1996).
8. T. Sasaki, T. Fukase, Phys. Rev. B **59**, 13872 (1999).
9. J. Wosnitza (private communication).
10. N. Harrison, C.H. Milke, D.G. Rickel, J. Wosnitza, J.S. Qualls, J.S. Brooks, E. Balthes, D. Schweitzer, I. Heinen, W. Strunz, Phys. Rev. B **58**, 10248 (1998).
11. M.A. Itskovsky, S. Askenazy, T. Maniv, I.D. Vagner, E. Balthes, D. Schweitzer, Phys. Rev. B **58**, R13347 (1998).
12. R. Peierls, Z. Phys. **81**, 186 (1933).
13. J. Wosnitza, S. Wanka, J. Hagel, E. Balthes, N. Harrison, J.A. Schlueter, A.M. Kini, U. Geiser, J. Mohtasham, R.W. Winter, G.L. Gard, Phys. Rev. B **61**, 7383 (2000).
14. M. Nakano, Phys. Rev. B **62**, 45 (2000).
15. K. Kishigi, Y. Hasegawa, M. Miyazaki, J. Phys. Soc. Jpn **68**, 1817 (1999).
16. A.S. Alexandrov, A.M. Bratkovsky, Phys. Rev. B **63**, 033105 (2001).
17. M.A. Itskovsky, T. Maniv, I.D. Vagner, Phys. Rev. B **61**, 14616 (2000).
18. M.A. Itskovsky, T. Maniv, I.D. Vagner, Z. Phys. B **101**, 13 (1996).
19. I.M. Lifshitz, M. Ya. Azbel, M.I. Kaganov, *Electron Theory of Metals* (Consultants Bureau, New York, 1973).
20. K. Kishigi, M. Nakano, K. Machida, Y. Hori, J. Phys. Soc. Jpn **64**, 3043 (1995).
21. Ju.H. Kim, S.Y. Han, J.S. Brooks, Phys. Rev. B **60**, 3213 (1999).
22. S.J. Han, J.S. Brooks, Ju.H. Kim, Phys. Rev. Lett. **85**, 1500 (2000).
23. D. Shoenberg, J. Low Temp. Phys. **56**, 417 (1984).
24. I.M. Lifshitz, A.M. Kosevich, Zh. Eksp. Teor. Fiz. **29**, 730 (1956) [Sov. Phys. JETP **2**, 636 (1956)].
25. E. Lifshitz, L. Pitaevsky, *Statistical Physics*, Part 2 (Pergamon, Oxford, 1986).
26. I.D. Vagner, T. Maniv, E. Ehrenfreund, Phys. Rev. Lett. **51**, 1700 (1983).
27. L. Ducasse, A. Fritsch, Solid State Commun. **91**, 201 (1994).
28. M.A. Itskovsky, G.F. Kventsel, T. Maniv, Phys. Rev. B **50**, 6779 (1994).
29. N. Harrison, E. Rzepniewski, J. Singleton, P.J. Gee, M.M. Honold, P. Day, M. Kurmoo, J. Phys. Cond. Matt. **11**, 7227 (1999).
30. N. Harrison, Phys. Rev. Lett. **83**, 1395 (1999).
31. T. Champel, V.P. Mineev, Phil. Mag. B **81**, 55 (2001).
32. P.D. Grigoriev, I.D. Vagner, `cond-mat/0009409` (26 Sept. 2000).
33. N. Harrison, R. Bogaerts, P.H.P. Reinders, J. Singleton, S.J. Blundell, F. Herlach, Phys. Rev. B **54**, 9977 (1996).